Probing the Ionosphere with the LWA by Rapid Cycling of Celestial Radio Emitters

Aaron Cohen (NRL) and Nagini Paravastu (NRL/ASEE)

March 12, 2008

ABSTRACT

Using knowledge of the low-frequency radio sky and the simulated observational capabilities of the Long Wavelength Array (LWA) we present a feasible method for the LWA to probe the overall structure of the ionosphere above the LWA. Such measurements could serve as the initial step in calibrating the ionospheric phases that distort astronomical images, thereby allowing the LWA to reach its full astrophysical potential. At the same time, it could generate a dynamic, all-sky model model of the ionosphere rich in phenomenology. This method consists of rapidly cycling through and imaging the several hundred celestial radio emitters (sources) that we predict will be isolated enough to be imaged with standard calibration techniques. Such sources can therefore function as ionospheric calibrators, because calibrating to them determines the differences in ionospheric column density (Total Electron Content differences, or ΔTEC) along the lines of sight from each LWA station towards each calibrator source. Our analysis, based on VLSS fluxes and LWA antenna simulations, show that, at 74 MHz, roughly 100 calibrator sources can be observed at any single time, which is far greater than the number of instantaneously available GPS or similar satellite beacons. With 52 stations, the LWA will be capable of probing at least 5,000 different lines of sight through the ionosphere. And with the effective collecting area of the LWA, we find that all available calibrator sources can be observed in well under 10 seconds. Implementation of this scheme requires that the LWA monitor and control system be capable of switching between sources on a 5-10 millisecond time scale.

1. Overview

The Long Wavelength Array (LWA) will observe celestial objects in the low-frequency radio spectrum (25-80 MHz) with unprecedented sensitivity and resolution. Additionally the LWA will be highly sensitive to small changes in ionospheric structure because small variations in the ionospheric column density (Total Electron Content, or TEC) produce relatively large phase distortions to incoming low-frequency radio waves. This presents both a challenge and an opportunity. The challenge is that in order for the LWA to achieve its astrophysical goals, it must measure and remove ionospheric phase distortions. An opportunity arises because, in doing so, large quantities of ionospheric data will necessarily be obtained with unique and potentially high scientific value.

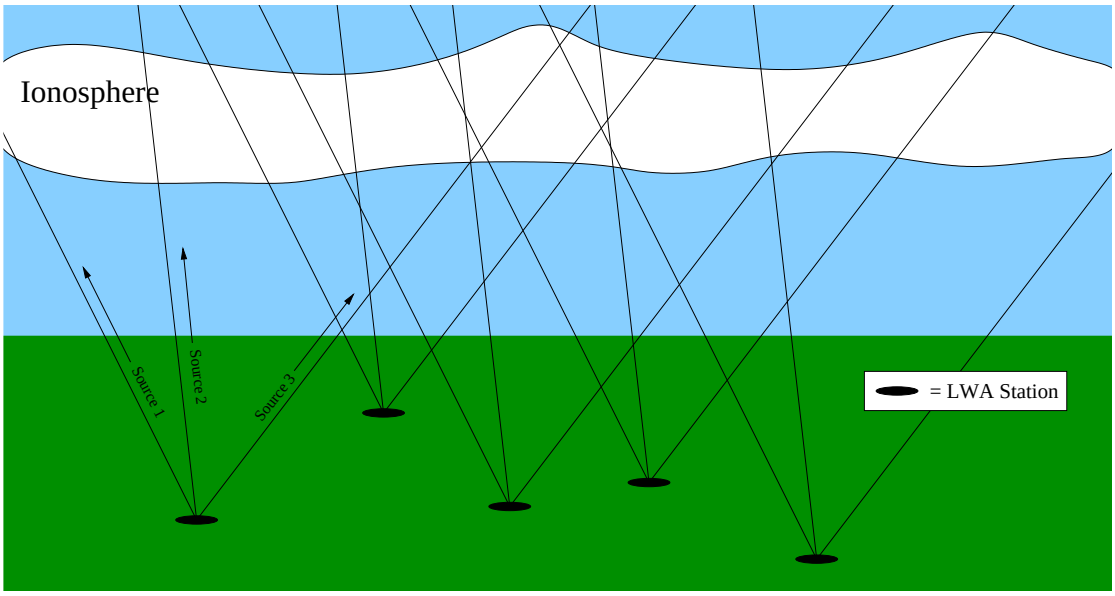

Fig. 1.— Schematic diagram showing the lines of sight toward 3 celestial radio sources from 5 LWA stations, for a total of 15 lines of sight through the ionosphere. The proposed scheme for measuring the ionosphere would have 52 stations rapidly scanning over 100 celestial radio sources measuring the ionosphere through over 5000 lines of sight.

Charged particles in the ionosphere cause a phase delay to incoming radio waves which is proportional to the TEC along the line of sight. An interferometer is not sensitive to a spatially constant phase delay, but is highly sensitive to variations in this phase delay between the interferometer elements. Calibration to a celestial radio source determines the relative phase delays between the interferometer elements. The measured phase delay is not necessarily the ionospheric phase delay, because it also may include delays caused by incorrect instrumental calibration and an integer number of 2π phase turns. However, the ionospheric phase delay varies as a strong and predictable function of observing frequency. Therefore, observations across a significant fractional bandwidth are needed to distinguish the ionospheric delays from other effects. The LWA will operate between 20 to 80 MHz with an instantaneous observing bandwidth of 8 MHz. Even at the upper end, from 72 to 80 MHz, where these measurements should be conducted, this fractional bandwidth should be sufficient. Once the ionospheric phase delays are known, it is straightforward to calculate the differences in the TEC (ΔTEC) along the lines of sight from each element towards that radio source.

Monitoring the phases toward many radio sources at once with an all sky monitor has been proposed as a possible calibration method for the LWA (Erickson 2005). In practice, an all sky monitor would be very difficult to implement because it would require cross correlation of all dipoles in the array (or at least the core) and it is not clear that sufficient resolution could be achieved over a field of view encompassing the entire sky. However, with the benefit of newly acquired

knowledge of both the low-frequency radio sky and LWA observing capabilities, we can now revisit this concept. Here we describe in detail a plausible, but somewhat different, method for achieving essentially the same thing. This calibration method consists of using the LWA in its normal imaging mode to rapidly cycle among many calibrator sources distributed throughout the sky. By rapid, we mean fast enough that the ionospheric structure doesn't change significantly. This would produce many ΔTEC measurements towards many different directions in the sky. The number of lines of sight that are probed is equal to the number of LWA stations times the number of radio sources that can be used as radio calibrators. As will be described in Section 2, we find that an average of just over 100 celestial calibrator sources are available at any time, and with 52 LWA stations, it is possible to probe well over 5,000 lines of sight through the ionosphere. From antenna simulations, which we describe in Section 3, we find that the LWA sensitivity is such that this can be done in well under 10 seconds. The height of maximum electron density in the ionosphere is typically about 350-400km, which, coincidentally, is also about the length of the longest baselines in the LWA. Because the calibrator sources are at a wide variety of positions in the sky, this will lead to a very comprehensive probing of the ionosphere above the LWA (Figure 1).

This method of ionospheric measurement should be done at the upper end of the 20-80 MHz frequency band in which the LWA will operate. This is because calibration works far better there because of the smaller field of view and much smaller ionospheric phase distortions. However, these measurements can be used for calibration of astronomical observations at any frequency. This is because one LWA "beam" (beam forming unit, or BFU) will be dedicated completely to ionospheric calibration (Clarke 2007). While that beam is measuring the ionosphere at 72-80 MHz, the observation "beam" can operate at any frequency, and the ionospheric measurements can be scaled to observing frequency.

While we present a detailed description of rapid cycling through ionospheric calibrators to probe the ionosphere, the specific use of these data both for scientific and calibration purposes requires further study. The purpose of this memo is to describe specifically what ionospheric data will be available to the LWA, how it can be collected, and the resulting requirements for the LWA monitor and control system. High spatial and time-resolution scanning of the ionosphere is a unique capability of the LWA that could yield exciting scientific results. Additionally, ionospheric calibration will be one of the greatest challenges to the operation of the LWA. Therefore it makes sense to design the LWA with the capabilities to collect all the ionospheric data that we show to be available.

2. Which Celestial Radio Sources Can Serve as Ionospheric Calibrators?

While most celestial radio sources will require full-field ionospheric calibration to image at the high resolution of the LWA, some sources are both bright enough and isolated enough that they dominate the flux density in their field of view to the extent that simple self-calibration is sufficient for imaging. Cohen et al. (2007a) used the recently completed 74 MHz sky survey (VLSS; Cohen

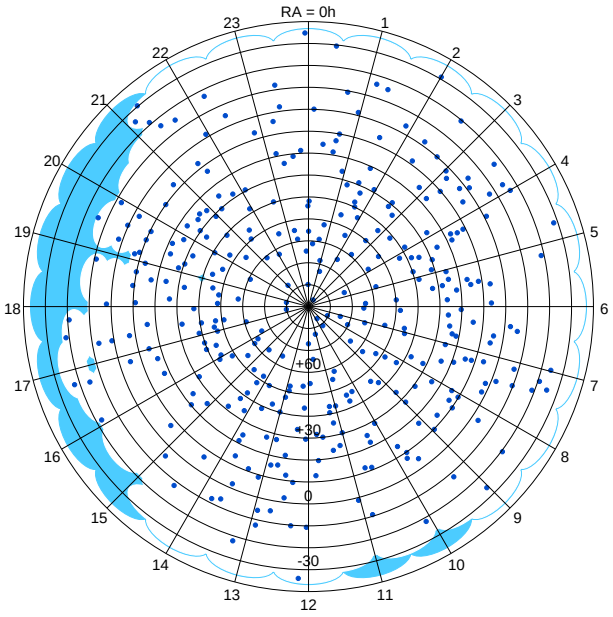

Fig. 2.— Locations (blue dots) of the 362 ionospheric calibrator sources identified using the VLSS (Cohen et al. 2007a). The shaded blue regions are the roughly 5% of the VLSS region remaining to be imaged.

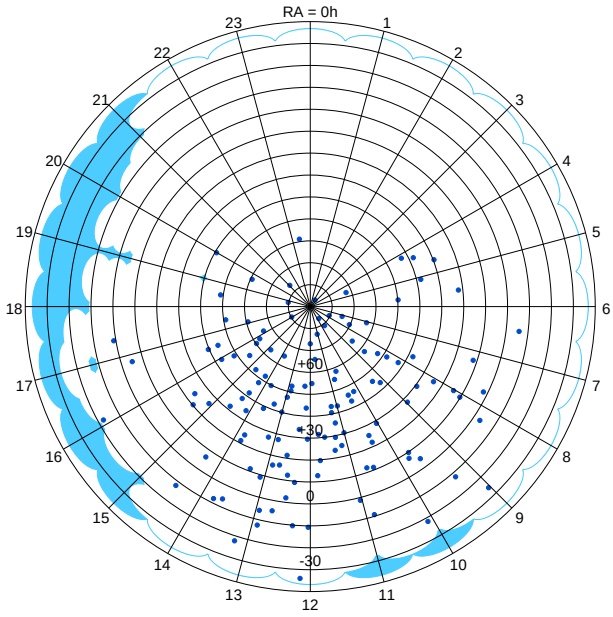

Fig. 3.— Locations (blue dots) of the 115 ionospheric calibrator sources that can be imaged at an LST of 12 hours.

et al. 2007b) to determine that there are 362 such sources in the sky visible to the LWA (roughly $\delta > -30°$)[1]. Such sources can be used to calibrate the LWA and thereby determine the ΔTEC between the stations in the direction of those sources. For this reason, we will refer to these 362 sources as ionospheric calibrators for the remainder of this memo. Figure 2 shows an all sky map of the identified ionospheric calibrators, which have an average spacing in the sky of about 9°.

These 362 ionospheric calibrators are all sources that can be imaged with self-calibration at *some* time during the day. For rapid scanning at a particular instant, we need to know how many of these ionospheric calibrators can be imaged at a specific time. At any given time, roughly half of the total number of ionospheric calibrators will be below the horizon. Additionally, some calibrators that are above the horizon cannot be imaged because they are at low elevation. The elevation of a source is important because the field of view, defined by the phased-array station beam, becomes elongated at low elevations. Significant elongation of the FOV can cause sources to no longer be isolated enough for self-calibration to work. In the analysis of Cohen et al. (2007a), the field of view used for each source was taken at the transit elevation of that source. This explains why the

[1]It was also determined that many more sources may be imaged with self-calibration if bandwidth smearing is used to suppress outlier sources, but to be conservative we concentrate on the source list that is imagable without the use of bandwidth smearing.

density of calibrator sources decreases at the far southern declinations as seen in Figure 2 – because even at transit, those sources have elongated fields of view, and so fewer are isolated enough within an LWA field of view to qualify as ionospheric calibrators.

For the current analysis, we calculated the number of ionospheric calibrators that are instantaneously available for imaging as a function of LST. As an example, Figure 3 shows the 115 sources that can function as ionospheric calibrators at LST = 12 hours. Through the full range of LST this number varies somewhat, but stays within the range of 99 to 123 sources, with an average value of 112 sources. In the next section, we estimate the amount of observing time needed for the LWA to image that many sources.

3. Time Required To Image All Available Ionospheric Calibrators

3.1. LWA Sensitivity

For an interferometric array of N elements, the rms noise level in an image is given by:

$$\sigma = \frac{2\,k_B\,T_{sys}}{\eta_s\,A_e\,\sqrt{N(N-1)N_p\,\Delta T\,\Delta\nu}} \tag{1}$$

where k_B is Boltzmann's constant, T_{sys} is the system temperature, η_s is the system efficiency, A_e is the effective collecting area of each station, N_p is the number of polarizations, ΔT is the observation time and $\Delta\nu$ is the frequency bandwidth. Thus the time required to achieve a given rms map noise (σ) is:

$$\Delta T = \frac{4\,k_B^2}{\eta_s^2\,N(N-1)N_p\,\Delta\nu}\left(\frac{A_e}{T_{sys}}\right)^{-2}\sigma^{-2} \tag{2}$$

For the full LWA we can assume $N = 52$ stations and $N_p = 2$ (dual polarization). Without complete knowledge of the system electronics, we conservatively estimate the system efficiency to be $\eta_s = 0.5$ (the VLA has $\eta_s = 0.78$). Although the LWA will have a total bandwidth of 8 MHz, we will need to measure the phase curvature across this bandwidth to separate the ionospheric phase delays from instrumental phase delays and 2π phase wraps. That will require that we measure the phases in small intervals across this bandwidth, and we take $\Delta\nu = 1$ MHz to be a reasonable estimate of the frequency resolution needed for this. The required rms map noise (σ) will depend on the brightness of each calibrator. For calibration to be effective, a signal-to-noise ratio of at least 10:1 is desired. But we also must anticipate that the peak brightness of a radio source at the much higher LWA resolution will be lower than that measured by the VLSS. Assuming most of the ionospheric calibrator sources are double lobed radio galaxies, we estimate the typical peak brightness at high resolution to be about half that measured in the VLSS. Therefore, to achieve 10:1 dynamic range, we require σ to be 1/20 times the VLSS peak brightness. That leaves only

Fig. 4.— A photograph a single-polarization tied fork antenna prototype.

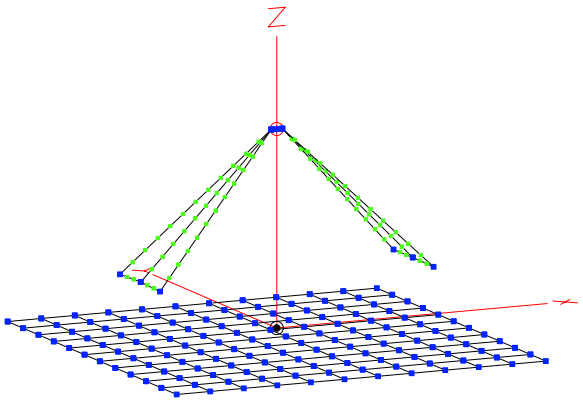

Fig. 5.— The NEC4 model of the single-polarization tied fork antenna over a 3 m × 3 m ground screen.

the ratio of the effective collecting area to the system temperature (A_e/T_{sys}) to be determined. This required antenna simulations, and the effective collecting area (A_e) is elevation dependent. We discuss this ratio in the next section.

3.2. Antenna Simulations

We simulated A_e/T_{sys} for a station of 256 dual polarization stands. We simulated a dual polarization 1.5 m Tied Fork antenna as this is likely to be either the actual antenna chosen or similar. A prototype of a single polarization 1.5 m Tied Fork is pictured in Figure 4. A model for this antenna, also shown in Figure 5, was simulated in NEC-4 at 74 MHz. In the model, the antenna feed point was positioned 1.5 m over a 3 m × 3 m ground screen on Earth ground. A dielectric constant of 13 and a conductivity of 0.005 S/m were used for the ground properties. Further detail on the modeling of this antenna will be provided in a future memo that is currently in preparation (Paravastu et al. 2008).

The effective area, A_e, of one dual polarization antenna is given by Equation 3, where λ is the wavelength in meters (4.03 m for 74 MHz). Γ is the reflection coefficient resulting from the impedance mismatch between the balun and the antenna feed point. L_g is the ground loss factor, and was determined by calculating the difference in antenna gain between real ground and perfect ground.

$$A_e = G_{tot}\frac{\lambda^2}{4\pi}\frac{(1-\Gamma^2)}{L_g} \tag{3}$$

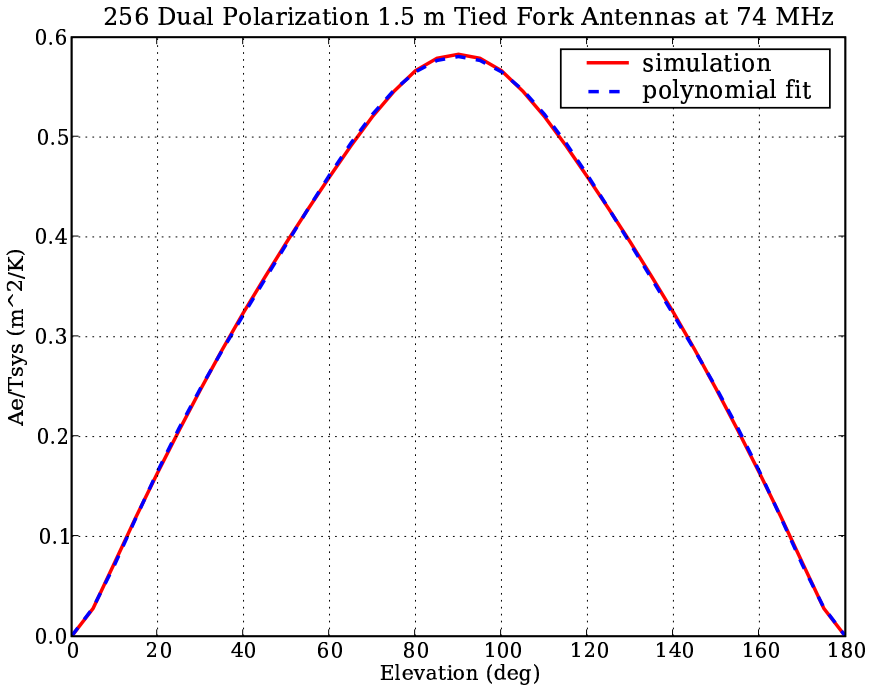

Fig. 6.— A_e/T_{sys} as a function of elevation for the dual-polarization tied fork antenna as determined through simulations. Values shown are for a station with 256 antennas.

G_{tot} is the total effective gain of a dual polarization stand used in an interferometer. For an interferometer measuring the total power in both polarizations, cross-polarization terms are not used and so the signal strength is equal to the quadratic sum of the signal at both polarizations. Therefore G_{tot} can be expressed by Equation 4, where $G_{E,1}$ is the E-plane gain of one polarization and $G_{H,2}$ is the H-plane polarization of the other.

$$G_{tot} = \sqrt{\frac{G_{E,1}^2 + G_{H,2}^2}{2}} \tag{4}$$

The system noise temperature, T_{sys} is given by Equation 5, where T_{sky} is the Galactic noise temperature and T_{balun} is the noise temperature of the antenna balun. T_{sky} was calculated using the Cane model (Cane 1979) and was found to be 1774 K at 74 MHz. For T_{balun}, the value for the LWDA and G250R baluns, which is 250 K, was used.

$$T_{sys} = T_{sky}\frac{(1-\Gamma^2)}{L_g} + T_{balun} \tag{5}$$

Using Equations 3 through 5 and NEC-4 to simulate the gains, we calculate A_e/T_{sys} as a function of elevation along the east-west azimuth for each antenna stand. Because of the 90° symmetry of a dual-polarization antenna, this is the same as along the north-south azimuth. While A_e/T_{sys} may vary somewhat off the N-S or E-W azimuths, for simplicity we applied the elevation dependence along these azimuths to all azimuths. For a full station of 256 antennas, we simply multiplied this value by 256, which does not take into account the effects of mutual coupling. However initial simulations show that the effect of mutual coupling changes the total collecting area by no more than about $\sim \pm 15\%$ for the combined E and H plane results (Ellingson 2007), and even this is likely to average out over many different directions in the sky. So this approximation should be sufficient for the purposes of this study.

The results are plotted in Figure 6. The effective collecting area reaches a maximum at zenith, with $A_e/T_{sys} = 0.583\ m^2/\mathrm{K}$. We created a polynomial fit to the data (also shown in Figure 6) so that we could estimate A_e/T_{sys} at the exact elevation of each source at a given time of day.

3.3. Time Required for Ionospheric Calibrator Scanning

Combining the LWA sensitivity equations from Section 3.1 with the A_e/T_{sys} simulations from Section 3.2, we can estimate the required observing time for a given ionospheric calibrator at a given elevation above the horizon. For example, the median peak brightness in the VLSS for the 362 ionospheric calibrator sources is 18.6 Jy/beam. Assuming that peak brightness falls by half at higher resolution means that one would need a sensitivity of $\sigma = 0.93$ Jy/beam to achieve 10:1 dynamic range. Using Equation 2 and the simulated collecting area (Figure 6), the observing time needed would be 20 milliseconds if that source is at zenith. However, if that same source is at an elevation of 35° above the horizon, the observing time becomes 83 milliseconds.

At any given time, a very small number of calibrator sources require a disproportionately long time to observe, because they are at a very low elevation. Therefore we did not include as "observable" any sources that require more than 200 milliseconds to observe, which greatly reduced the total observing time while only slightly reducing the total number of sources. Also, while some sources are bright enough and have a high enough elevation to be observed in 1 milliseconds or less, we require each source to be observed for at least 10 milliseconds. This has negligible effect on the total observing time, while allowing for the fact that the instrument might require this much time to stabilize. Thus each source will be observed for between 10 to 200 milliseconds.

Figure 7 shows the number of observable ionospheric calibrators at each hour of LST. This varies from 99 to 123 with an average of 112. We have also calculated and summed the total observing time required to image all observable ionospheric calibrators at each hour of LST, which is also included in Figure 7. This varies between 3.8 and 6.6 seconds, with an average of 5.3 seconds. The average observing time per source is about 50 milliseconds.

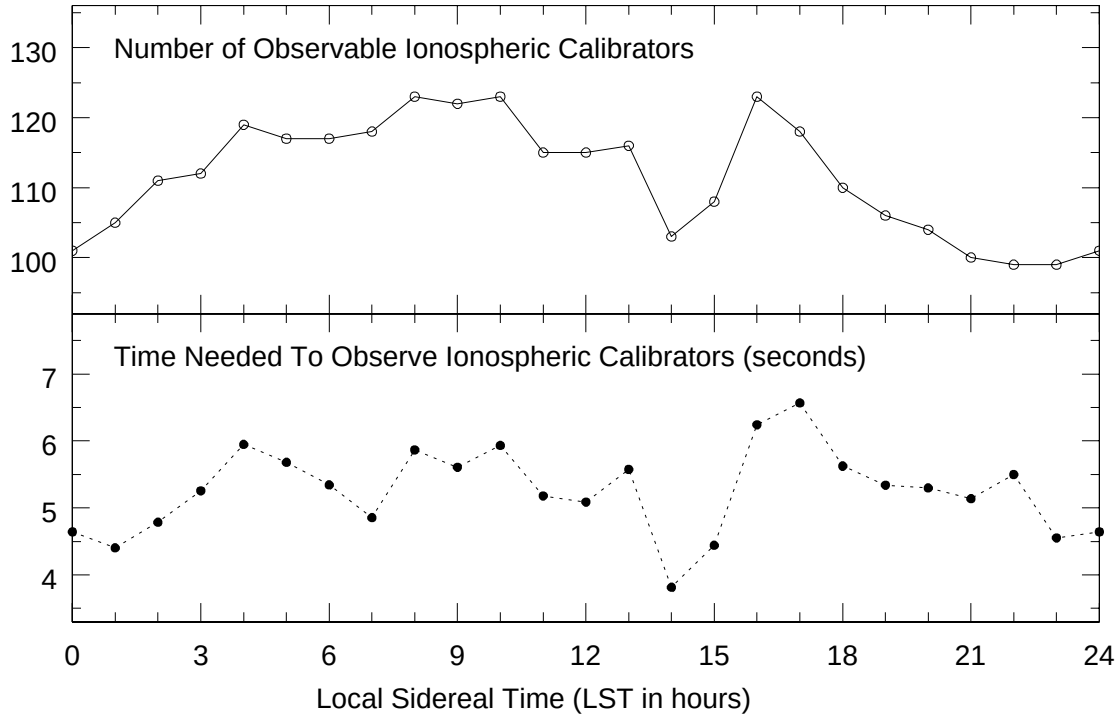

Fig. 7.— Number of observable ionospheric calibrators (top) and the total observing time required to achieve 10:1 dynamic-range images of them all (bottom) plotted as a function of local sidereal time (LST) at the LWA.

3.4. Requirements for LWA Monitor and Control System

Of course the time required to scan all available ionospheric calibrators is not just the total observing time, but also the time needed to switch between sources. A significant advantage of the LWA is that it can change its observing direction without any physical movements such as slewing of antenna dishes. Instead this is done electronically by changing the geometrical delays between elements. The time required to calculate and change these delays and begin observing a new source is considered "overhead" time. A reasonable amount of overhead time is generally about 10-20%, and so the electronics should be designed to switch between sources on about a 5-10 millisecond time scale, which would extend the average 5.3 seconds of observing time to about 6.5 seconds including source switching. If switching between sources were to be much slower than this it would significantly slow the scanning speed, and hence the ability to probe the ionosphere on fast enough timescales for useful calibration and scientific studies.

4. Results and Discussion

Calibration to an ionospheric calibrator source accurately determines the relative phases at each LWA station, which can be used to determine the ΔTEC between each station in the direction of that source. With 52 stations, and an average of 112 available ionospheric calibrators, this gives the ΔTEC for 5,772 lines of sight. Collecting area simulations show that these lines of sight can all be probed in an average of about 5.3 seconds, or about 6.5 seconds including reasonable "overhead" time for source switching.

If we approximate the ionosphere as a "thin screen", we can estimate the density of pierce points in the sky where each line of sight crosses the 2-dimensional screen. Although the LWA will have 52 stations spread over a $\sim$400 km region, about 15 of these will be concentrated inside a $\sim$10 km core (Cohen 2006). Because its pierce points will be close enough that they measure nearly the same line of sight, the core is best treated as if it were a single station for this calculation. That leaves 38 stations times $\sim$100 calibrator sources, or about 3800 independent pierce points. Most observable calibrators have an elevation above the horizon of at least 30°, and if we divide that sky area by the number of pierce points, we estimate an average angular distance between pierce points of 1.6°. The LWA field of view is about 2.5° at 80 MHz, and about 10° at 20 MHz. Therefore the density of pierce points will possibly provide enough calibration information at the low end of the LWA frequency range, but probably not at the high end. However this method is only intended to probe the (relatively) large scale structure as a first step in the ionospheric calibration. From that calibration starting point, progressively fainter sources within the field of view should become visible, and can be used to measure and calibrate the finer scale ionospheric structure in a manner similar to field-based calibration which is currently used for the 74 MHz VLA (Cotton et al. 2004).

At zenith, and for a $\sim$ 400 km screen height, a pierce point every 1.6° corresponds to roughly one pierce point every $\sim$11 km, though this density declines far from zenith. This will provide a much higher resolution map of the ionosphere than current methods such as GPS measurements provide. While a 2-dimensional "thin screen" model of the ionosphere would certainly provide interesting science, with this many lines of sight, one can also begin to imagine a complete 3-dimensional tomographic reconstruction of the ionosphere. The main caveat for both cases is that the lines of sight only measure *differences* in TEC among stations toward source locations. This results in a degeneracy consisting of an unknown and different reference phase for each set of lines of sight to each ionospheric calibrator source. Overall that results in about 100 unknown parameters plus probably several hundred parameters needed to produce a high resolution all-sky model of the ionosphere. That would still be an over-determined system given that there are 3800 independent measurements. Additionally, the availability of independent TEC measurements, e.g. via GPS receivers embedded throughout the array, coupled with physical continuity constraints could add further constraints. Therefore the degeneracy in absolute TEC values is, in this case, potentially quite solvable, though the exact mechanism remains a subject for future investigation.

REFERENCES

Cane, H. V. 1979, MNRAS, 189, 465

Clarke, T. E. "Scientific Requirements for the Long Wavelength Array Ver. 2.3", Long Wavelength Array Memo #117, Nov 19, 2007 (SRR approved version)

Cohen, A., "A Potential Array Configuration for the LWA", Long Wavelength Array Memo #55, September 29, 2006.

Cohen, A., Clarke, T. & Lazio, J. "Early Science from the LWA Phase II: A Target List", Long Wavelength Array Memo #80, February 12, 2007a.

Cohen, A. S., Lane, W. M., Cotton, W. D., Kassim, N. E., Lazio, T. J. W., Perley, R. A., Condon, J. J., & Erickson, W. C. 2007b, AJ, 134, 1245

Cotton, W. D., Condon, J. J., Perley, R. A., Kassim, N., Lazio, J., Cohen, A., Lane, W., & Erickson, W. C. 2004, Proc. SPIE, 5489, 180

Ellingson, S. "Effective Aperture of a Large Pseudorandom Low-Frequency Dipole Array", Long Wavelength Array Memo #73, Jan 13, 2007 and 2007 IEEE Int'l Ant. & Prop. Symp., Honolulu, HI

Erickson, W. C. 2005, Astronomical Society of the Pacific Conference Series, 345, 317

Paravastu, N., Erickson, W. & Hicks, B. "Comparison of Antenna Designs on Groundscreens for the Long Wavelength Array" (LWA Memo in prep)

Taylor, G. et al. "LWA Overview", Long Wavelength Array Memo #56, September 22, 2006.

This preprint was prepared with the AAS LaTeX macros v5.2.